

## DEVELOPMENT AND COMMISSIONING OF THE K500 SUPERCONDUCTING HEAVY ION CYCLOTRON\*

Sumit Som<sup>†</sup>, Arup Bandyopadhyay, Samit Bandyopadhyay, Sumantra Bhattacharya, Pranab Bhattacharyya, Tamal Kumar Bhattacharyya, Uttam Bhunia, Niraj Chaddha, Jayanta Debnath, Malay Kanti Dey, Anjan Dutta Gupta, Surajit Ghosh, Aditya Mandal, Paris Yalagoud Nabhiraj, Chinmay Nandi, Md. Zamal Abdul Naser, Sandip Pal, Sarbajit Pal, Umashankar Panda, Jedidiah Pradhan, Anindya Roy, Subrata Saha, Sudeshna Seth, Sajjan Kumar Thakur  
VECC, Variable Energy Cyclotron Centre, Kolkata, India

### Abstract

The K500 Superconducting Cyclotron (SCC) has been developed indigenously and commissioned at VECC. The three-phase Radio-Frequency (RF) system of SCC, consists of three half-wave cavities placed vertically 120 deg. apart. Each half-wave cavity has two quarter-wave cylindrical cavities tied together at the centre and symmetrically placed about median plane of the cyclotron. Each quarter-wave cavity is made up of a short circuited non-uniform coaxial transmission line (called "dee-stem") terminated by accelerating electrode (called "Dee"). The SCC, operating in the range 9 to 27 MHz, has amplitude and phase stability within 100 ppm and 0.1 deg. respectively. The overview of all the subsystems of the cyclotron along with low-level RF (LLRF), high and low power RF amplifiers, cavity analysis, absolute Dee voltage measurement using X-ray method, amplitude and phase control loops will be presented in the talk. The commissioning of the cyclotron with first harmonic Nitrogen<sup>4+</sup> beam extracted at 252 MeV, while operating at 14 MHz RF frequency, along with the correction of first harmonic magnetic field error by repositioning the cryostat within 120 micron accuracy, will be discussed briefly.

### INTRODUCTION

The Variable Energy Cyclotron Centre (VECC) at Kolkata, India, has been focused on building cyclotrons as a tool for nuclear physics experiments and medical applications. The center has developed a K130 cyclotron with normal conducting coils and a K500 cyclotron with superconducting coils. Also, VECC has been operating IBA-make 30MeV Medical Cyclotron from production of radioisotopes.

Recently, the first harmonic Nitrogen<sup>4+</sup> beam of 18 MeV/A was extracted from the K500 SCC (as shown in Fig. 1). A 14 GHz Electron Cyclotron Resonance (ECR) ion source (Fig. 2) is integrated with the cyclotron using 28 meters long low energy beam transport line. Initially, the internal beam could be accelerated up to the extraction radius, but could not be extracted due to imperfection of ~50 Gauss of 1<sup>st</sup> harmonic magnetic field ( $B_1$ ) at the extraction region prohibiting the beam's extraction. The root cause of the imperfection was a damaged dowel resulting in erroneous position of the coil and cryostat. The

machine was dismantled and corrected. Subsequently, the coil and cryostat were repositioned with an accuracy within 120  $\mu\text{m}$ , by devising a new positioning mechanism for precise radial movement of the cryostat. Three radial screws were used to move the 12 Tonnes cryostat. Dial gauges at the outer radius of the cryostat were used to estimate the movement of the cryostat. The final measurement of the cryostat position was taken with a portable CMM machine. Extensive mapping of magnetic field at different excitations of primary coils was carried out. The gross reduction of the imperfection of  $B_1$  achieved to ~7 Gauss at extraction radius resulted in successful extraction of the beam.



Figure 1: The K500 superconducting cyclotron at VECC.



Figure 2: 14GHz ECR ion source and injection beam line.

\* Work supported by the DAE, Government of India.

<sup>†</sup> email: [ssom@vecc.gov.in](mailto:ssom@vecc.gov.in)

The superconducting cyclotron consists of several challenging technologies that took a considerable time to prepare for the operation, e.g., the NbTi (niobium-titanium) wired magnet, the cryogenic system, the cryo-panel-cooled vacuum system, independently driven three-dee radio-frequency acceleration system, compact magnetic field mapping system, compact electrostatic deflectors, etc.

## SUPERCONDUCTING MAGNET

The main component of the K500 superconducting cyclotron is a pill-box type dipole magnet, with a cylindrical iron structure energized by NbTi coil, operating at liquid 4.2K. It produces high magnetic field (up to 5 Tesla) to bend the charge particle beams in a near-circular orbit, which spirals out as energy of the beam increases. The superconducting cyclotron has  $K_{\text{bend}}=520$  and  $K_{\text{foc}}=160$ . The basic design of the machine is based on the superconducting cyclotrons built at Michigan State University and Texas A&M University in USA [1, 2, 3].

### Iron Frame

The magnet frame is a cylindrical pill-box structure made of about 80 Tonnes of low carbon magnetic steel (AISI 1020), as shown in Fig. 3. The magnet poles are attached to the circular end-plates at the top and bottom. The outer ring (yoke) supports the end plates and serves as the magnetic flux return path. The coil sits in the annular space between the return path and the poles. The poles are of 0.654 meter radius. Both the poles have three spiral hills, each covering an angle of  $46^\circ$  at the outer radii. The average spiral constant is  $(1/33.02)$  rad/cm. The gap

between the upper and lower hills is 64 mm. The valley regions between the adjacent hills have much more significant gaps, varying radially in three steps. These hill-valley structures create the necessary azimuthal variation of the magnetic field. The whole structure has median-plane reflection symmetry. The magnet iron frame is 3.048 meters in diameter and 2.2 meters in height. It is installed on three piers levelled within an accuracy of  $800 \mu\text{m}$ . The lower and the upper half of the magnet iron pole are shown in Fig. 3.

### Superconducting Coil and Cryostat

The cryostat sits in the annular space between the pole and the return yoke (from 0.654 meter to 1.066 meter radius). It houses the two pairs of independently powered superconducting coils, usually called the  $\alpha$  coil and the  $\beta$  coil. The coils are made of NbTi multifilament composite superconducting cable (with critical current 1030 A at 5.5 Tesla and 4.2 K), consisting of 500 filaments of 40 micron diameter embedded in the copper matrix (in 1:20 ratio). The superconducting coils are wound on a bobbin made from stainless steel (SS316L). Annular Stainless Steel (SS) sheets are welded to the top and bottom edges of the bobbin all along the periphery to form the liquid-helium chamber containing the coils to cool them down at 4.2 K for cryogenic stability. It is then wrapped with several multi-layer insulation (MLI) sheets. A liquid-nitrogen (LN) cooled thermal shield made of copper sheets encloses the liquid-helium chamber. Several layers of MLI wrappings are provided outside the LN-shield also. The entire coil assembly is then inserted into an annular magnetic steel chamber called coil-tank, as shown in the Fig. 4.



Figure 3: Different parts of iron frame of the magnet: lower half of the magnet (at top-left), three spiral hills (at top-right), return yoke ring (at bottom-left), upper half of the magnet (at bottom-right).

Content from this work may be used under the terms of the CC BY 4.0 licence (© 2022). Any distribution of this work must maintain attribution to the author(s), title of the work, publisher, and DOI



Figure 4: Different parts of cryostat and coil assembly: bobbin made of Stainless Steel (at top-left), Coil-winding machine (at top-middle), superconducting primary coils (at top-right), Copper made liquid nitrogen cooled radiation shield (at bottom-left), MLI wrapped coil plus shield being inserted into the cryostat vacuum chamber made of magnetic steel (at bottom middle), Coil tank with its radial inserts being installed on magnet (at bottom-right).

Nine glass-epoxy support links keep the coil suspended inside the coil tank, three from the top, three from the bottom and three in radial directions. By adjusting the tension in these supports, the coil position is changed. Twenty radial penetrations are welded on the outer surface of the coil tank at the median plane to insert the drives for electrostatic deflectors and magnetic channels, beam diagnostic elements, etc. Cryogenic lines and the power feed-throughs are connected from the top. The cryostat is installed on the lower part of the magnet structure and the upper half of the magnet is lowered down on it using a motorized system to complete the installation. One needs to raise the upper half to access the cyclotron beam chamber.

### Trim Coils

Thirteen numbers of field trimming copper coils are wound around each of the six spiral pole-tips (as shown in Fig. 5). All these 78 numbers of trim coils are made of water-cooled copper conductor. The leads of these coils penetrate through the circular holes in the magnet end-plates. All the six trim coils at a particular radius – the upper and lower pairs in all three sectors – are connected in series, except the innermost and outermost trim coils. In case of these two, coils of individual sectors are powered independently, so that they can be used to produce harmonic fields other than 3N harmonics (N=3) and average field contribution. There is a circular trim coil mounted on the central-plug.



Figure 5: The trim coils are mounted on the pole tip and then vacuum impregnated with epoxy resin.

### RF Acceleration System

The RF cavity (as shown in Fig. 6) of K500 superconducting cyclotron (SCC) at VECC consists of three half-wave ( $\lambda/2$ ) cavities placed vertically 120 degree apart. Each half-wave cavity [4] has two quarter-wave ( $\lambda/4$ ) cylindrical cavities tied together at the centre and symmetrically placed about median plane of the cyclotron. Each quarter-wave cavity is made up of a short circuited non-uniform coaxial transmission line (called "dee-stem") terminated by accelerating electrode (called "Dee"). The RF cavity is analysed using 3D CST Microwave Studio code and RF parameters like Shunt impedance, Quality factor and cavity size etc. have been calculated in the operating frequency range of 9–27 MHz. During the

commissioning of RF system, absolute Dee voltage calibration has been done by using AMPTEK make CdTe (Cadmium Telluride) X-ray detector and the calculated RF parameters have been validated by the measured absolute Dee voltage [5], RF power and quality factor of the cavity.

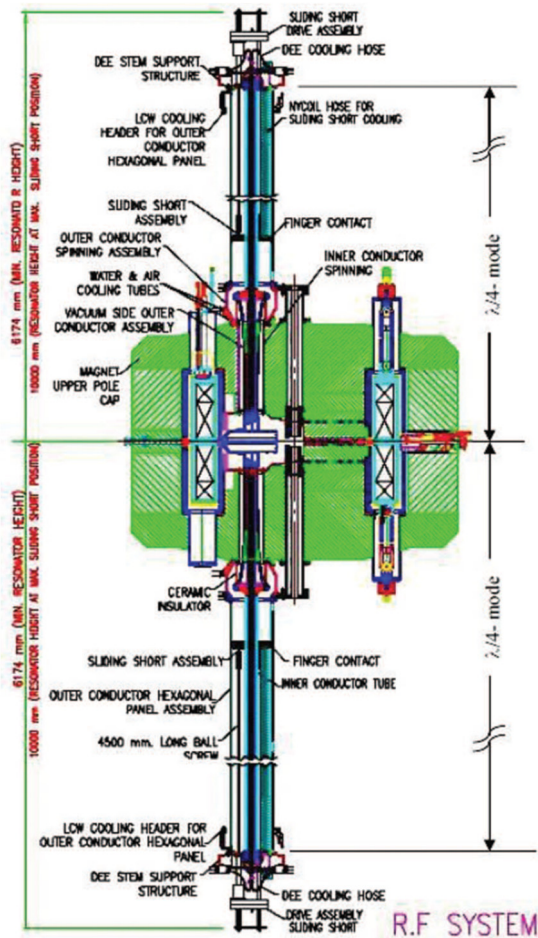


Figure 6: Half-wave coaxial RF cavity of SCC.

The phase control system has the option to change the relative phase difference between any two RF cavities and maintain the phase stability [6] within  $\pm 0.1^\circ$  during round-the-clock cyclotron operation. The said precision phase loop consists of both analog In-phase/Quadrature (I/Q) modulator to achieve faster response and also Direct Digital Synthesis (DDS) based phase shifter to achieve wide dynamic range as well. Three spiral Dees are situated in the three spiral valley regions (as shown in Fig. 7). Dee-stem consists of uniform coaxial line (in air) and also tapered line (in vacuum). The sliding short plate is electrically connected to the outer and inner conductors of coaxial line by Be-Cu contact finger with silver-graphite (99% silver +1% graphite) contact balls at the tip.

Each of the three half-wave cavity is fed with rf power (80 kW max.) from each of the three high power tetrode based final RF amplifiers (as shown in Fig. 8), developed in-house. RF system of SCC has been operated at 14 MHz with dee voltage in the range of 45 - 50 kV, to extract the first harmonic 252 MeV Nitrogen<sup>4+</sup> and 360 MeV Neon<sup>6+</sup> beam.



Figure 7: Lower dees and Liner.

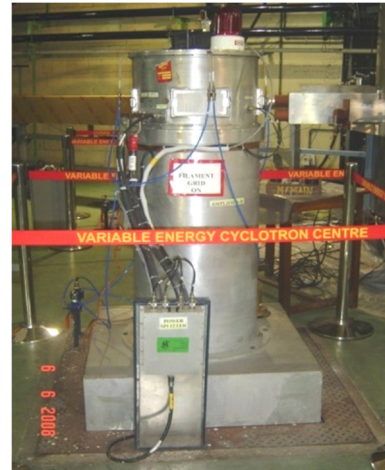


Figure 8: Tetrode based final RF Amplifier.

### Magnetic Field Mapper

The magnetic field was mapped with a search coil and NMR set up on a polar  $(r, \theta)$  grid at the median plane of cyclotron with 0.1-inch radial step and  $1^\circ$  azimuthal step. The mechanical system comprises of a cantilever arm assembly, the radial drive assembly, angular drive and transducer assembly. The arm assembly consists of a straight track, a support bar, a cart carrying the search coil and a linear encoder. All materials of the arm assembly, placed inside the cyclotron, are non-metallic and non-magnetic to avoid distortion because of the high magnetic field and eddy current forces on them. A linear encoder made of a photo sensor assembly head that moves on a linear optical strip with 360 lines/inch was used to measure the radial position of the search coil during mapping. A drive mechanism consisting of a DC brush-less servo motor, spur-gear set and a pulley-drum was used to move the search coil radially at a uniform velocity of about 40 cm/sec. A Kevlar string wound on the pulley-drum was connected to the search coil through the hollow angular drive shaft. The search coil moved from -50 mm to 685 mm on the base track along the radial direction of the cyclotron. The zero (0 mm) in this scale represents the mapping centre. One out of every thirty-six pulses from the encoder was used to trigger the digital integrator unit to read and integrate the search coil output between two successive triggers. After completing each radial scan for a particular angular position, the arm assembly was rotated

Content from this work may be used under the terms of the CC BY 4.0 licence (© 2022). Any distribution of this work must maintain attribution to the author(s), title of the work, publisher, and DOI

in  $1^\circ$  or  $0.5^\circ$  angular steps using an angular drive mechanism. The angular position of the search coil carrying arm is determined by an absolute rotary Inductosyn encoder with an accuracy of 1.7 arc-sec, which was obtained using two dual channel preamplifier and AWICS converter board. A micro-controller based interface module was used to read the angular position online.

## COMMISSIONING

### Magnetic Field Correction

The mapping system consists of a search coil that moves on a radial track with an optical sensor mounted on the coil cart. The counts in the digital integrator were calibrated using two absolute field values by a Nuclear Magnetic Resonance (NMR) probe placed at the center of the machine and in specific hill and valley locations, where the field uniformity meets the requirement of NMR locking. The  $360^\circ$  polar map covers a radius of 668 mm with a radial and azimuthal step size of 2.54 mm and  $1^\circ$ , respectively. The linear encoder that provides the position of the search coil has an accuracy of 10  $\mu\text{m}$ . The measurement accuracy of the angular encoder is 1.7 arc sec.

Positioning the coil-tank and coils coaxially with the iron mass is a significant concern in K500 superconducting cyclotron since it introduces 1<sup>st</sup> harmonic field imperfection in the extraction region cyclotron [7, 8]. It is undesirable because the equilibrium orbit (EO) is off-centered due to 1<sup>st</sup> harmonic field imperfections as the beam passes through  $\nu_r = 1$  resonance. In K500 SCC, the beam passes through  $\nu_r = 1$  resonance near the machine's center and again near the extraction zone. The stable regions of phase space also shrink to zero at these resonance zones. In addition, the off-centering of the orbit may excite the critical Walkinshaw resonance ( $\nu_r = 2\nu_z$ ) resulting vertical blow-up of the beam.

About 28 Gauss 1<sup>st</sup> harmonic field in the central region and 50 Gauss in the extraction region were observed (Fig. 9). The first harmonic peaks show an iron-produced component nearly independent of coil excitations. The 1<sup>st</sup> harmonic field introduced due to misalignment of the superconducting coils was current dependent, as in the radial range from 400 mm to 600 mm. The peak near 650 mm radius was due to positioning error of the coil-tank.

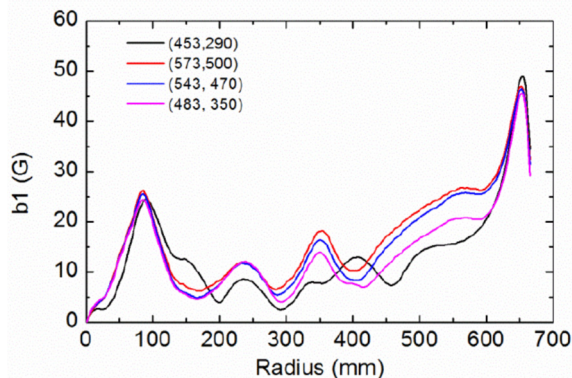


Figure 9: The 1<sup>st</sup> harmonic field amplitude vs. radius.

The 1<sup>st</sup> harmonic field near centre was reduced below 10 Gauss by a suitable trimming of iron in large-hill-addition, as shown in Fig. 10.

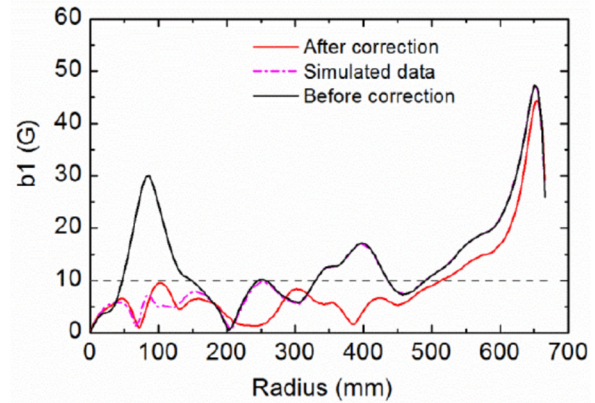


Figure 10: 1<sup>st</sup> harmonic amplitude ( $I_\alpha = 453\text{A}$ ,  $I_\beta = 290\text{A}$ ) before and after correction of large-hill-addition.

It was noted that the optimum coil position to minimize 1<sup>st</sup> harmonic component might increase the radial force on the support links. Therefore, keeping the coil in a compromised place was necessary. Following the careful repositioning of the coil and the coil tank with an accuracy of  $\pm 100.0\ \mu\text{m}$ , the measured 1<sup>st</sup> harmonic field amplitude reduced below 10 Gauss, as shown in Figs. 11 and 12.

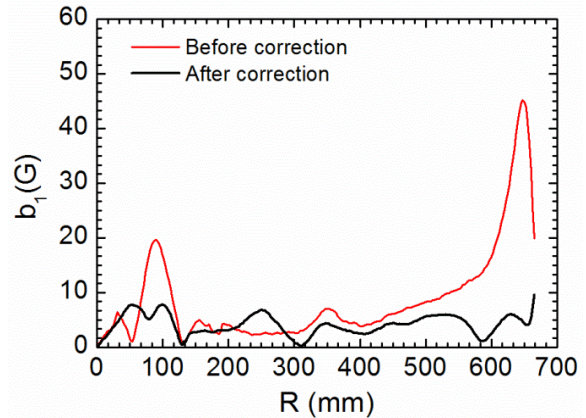


Figure 11: 1<sup>st</sup> harmonic field before and after correction of cryostat position.

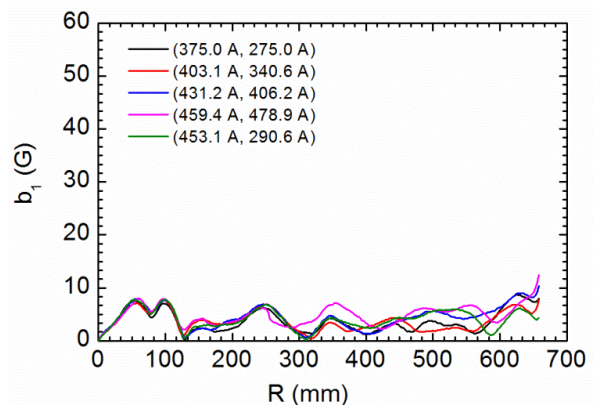


Figure 12: 1<sup>st</sup> harmonic amplitude at different excitations of main coils.

## BEAM EXTRACTION

The magnetic field correction led to successful extraction of the beam from K500 SCC at VECC [9–12]. Isochronous field fitting code TCFIT was used to calculate the current settings of 2 main coils and 14 trim coils using the measured magnetic field data. Nitrogen<sup>2+</sup> beam at 4.5 MeV/u in 2<sup>nd</sup> harmonic mode of operation and Nitrogen<sup>4+</sup> beam at 18 MeV/u in 1<sup>st</sup> harmonic mode of operation are extracted from the cyclotron and transported to the experimental cave. The profile of accelerated and extracted beam current is shown in Fig. 13.

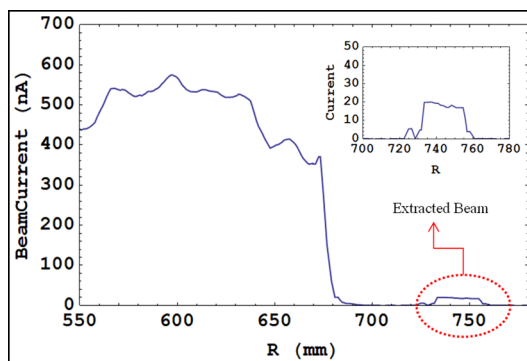


Figure 13: Beam current vs. radius for N<sup>2+</sup>, 4.5 MeV/u beam ( $f_{rf} = 14$  MHz, in 2<sup>nd</sup> harmonic mode of operation); First deflector entry was at 668.0 mm.

## ACKNOWLEDGEMENTS

I am thankful to VECC scientists, engineers and technical staff who have put their relentless effort in successfully extracting the second and first harmonic beam from K500 superconducting cyclotron.

## REFERENCES

- [1] H. G. Blosser, “The Michigan State University superconducting cyclotron program”, *IEEE Trans. on Nucl. Sci.*, vol. 26, no. 2, p. 2024, Apr. 1979.  
doi:10.1109/TNS.1979.4329804
- [2] D. P. May *et al.*, “Status of the Texas A&M K500 Superconducting Cyclotron”, in *Proc. 10th Int. Cyclotron Conf. and Their Applications (Cyclotrons'84)*, East Lansing, MI, USA, Apr.-May 1984, paper F05, pp. 267-270.
- [3] R. K. Bhandari, “Status of the Calcutta K500 Superconduction Cyclotron Project”, in *Proc. 16th Int. Conf. on Cyclotrons and Their Applications (Cyclotrons'01)*, East Lansing, MI, USA, May 2001, paper C-4.

- [4] S. Som *et al.*, “Development Of Rf System For K500 Superconducting Cyclotron at VECC Kolkata”, in *Proc. 18th Int. Conf. on Cyclotrons and Their Applications (Cyclotrons'07)*, Giardini-Naxos, Italy, Oct. 2007, pp. 473-475.
- [5] Sumit Som, Sudeshna Seth, Aditya Mandal, Saikat Paul, Anjan Duttagupta, “Radio frequency cavity analysis, measurement and calibration of absolute Dee voltage for K500 superconducting cyclotron at VECC, Kolkata”, *Rev. Sci. Instrum.*, vol. 84, p. 023303, 2013.  
doi:10.1063/1.4789784
- [6] Sumit Som, Surajit Ghosh, Sudeshna Seth, Aditya Mandal, Saikat Paul, Suprakash Roy, “Precision phase control for the radio frequency system K500 superconducting cyclotron at Variable energy Cyclotron Centre, Kolkata”, *Rev. Sci. Instrum.*, vol. 84, p. 113303, 2013.  
doi:10.1063/1.4828670
- [7] M. K. Dey *et al.*, “Coil Centering Of The Kolkata Superconducting Cyclotron Magnet”, in *Proc. 18th Int. Conf. on Cyclotrons and Their Applications (Cyclotrons'07)*, Giardini-Naxos, Italy, Oct. 2007, pp. 438-440.
- [8] F. Marti and P. S. Miller, “Magnetic Field Imperfections in the K500 Superconducting Cyclotron”, in *Proc. 10th Int. Cyclotron Conf. and Their Applications (Cyclotrons'84)*, East Lansing, MI, USA, Apr.-May 1984, paper B25, pp. 107-110.
- [9] J. Debnath, U. Bhunia, M. K. Dey, J. Pradhan, A. Dutta, S. Paula, A. Dutta Gupta, A. Bandyopadhyay and S. Som, “Optimization of compensation of magnetic field imperfection in K500 superconducting cyclotron”, *J. Instrum.*, vol. 15, no. 9, Sep. 2020.  
doi:10.1088/1748-0221/15/09/t09004
- [10] J. Pradhan, J. Debnath, M. K. Dey *et al.*, “Median plane and Beam Diagnosis in the Central region for Compact Superconducting Cyclotron”, *Nucl. Instrum. Methods Phys. Res., Sect. A*, vol. 993, p. 165084, Mar. 2021.  
doi:10.1016/j.nima.2021.165084
- [11] J. Pradhan, J. Debnath, M. K. Dey, *et al.*, “Characteristics of beam loss in compact superconducting cyclotron”, *J. Instrum.*, vol. 15, Aug. 2020.  
doi:10.1088/1748-0221/15/08/T08006
- [12] S. Paul, U. Bhunia, J. Debnath, M. K. Dey *et al.*, “A beam dynamics study for efficient extraction from the VECC K500 superconducting cyclotron”, accepted in *J. Instrum.*, Mar. 2022.  
doi:10.1088/1748-0221/17/03/P03029